

# EXTRACTION, TRANSPORT AND COLLIMATION OF THE PSI 1.3 MW PROTON BEAM

D. Reggiani<sup>#</sup>, Paul Scherrer Institut, 5232 Villigen PSI, Switzerland

## Abstract

With an average operating beam power of 1.3 MW the PSI proton accelerator complex is currently leading the race towards the high intensity frontier of particle accelerators. This talk gives an overview of the extraction of the 590 MeV beam from the ring cyclotron and its low loss transport to the meson production targets M and E as well as to the SINQ spallation neutron source. Particular regard is given to the collimator system reshaping the beam which leaves the 40 mm thick graphite target E before reaching SINQ. Since 2011, up to 8 second long beam macro-pulses are regularly diverted to the new UCN spallation source by means of a fast kicker magnet. The switchover from the SINQ to the UCN beam line as well as the smooth beam transport up to the UCN spallation target constitute the subject of the last part of the talk.

## INTRODUCTION

The PSI high intensity proton accelerator (HIPA) generates a continuous wave (50.6 MHz frequency) 590 MeV, 1.3 MW beam [1]. A schematic of the accelerator complex is shown in Fig. 1. Protons are provided by an ECR source, brought to 870 keV energy by a Cockcroft-Walton generator and then transferred through a LEBT-section to the 72 MeV injector cyclotron. The medium energy beam is transferred to the 590 MeV ring cyclotron. Losses occurring at the ring extraction are the most common limiting factor for the beam intensity. Indeed, in order to avoid unsustainable machine activation, the extraction losses have to be kept within the

lower  $10^{-4}$  range. The 1.3 MW beam is transported to a first 5 mm thick meson production graphite target (M) where 1.6% of the beam is lost. A second 40 mm thick graphite target (E) is mounted some 18 m downstream. About 12% of the beam is lost on the target itself while an additional 18% of it is absorbed by a powerful collimator system that reshapes the highly divergent beam and at the same time protects accelerator components from activation. The remaining beam is eventually transported to the SINQ neutron spallation source where it is completely absorbed. In case of a SINQ technical stop, the HIPA facility can still run at about 1 MW beam power (75% of the nominal intensity) thanks to a beam dump installed downstream of target E. A total of seven muon or pion secondary beam lines are located at the meson production targets M and E while SINQ provides neutrons for eighteen beam lines.

In 2011 the UCN neutron source was brought into routine operation at HIPA [2]. This second spallation source runs concurrently to SINQ and is driven by 1.3 MW proton macro-pulses kicked into the UCN beam line with a maximum duty cycle of 1%. The switchover of a megawatt class beam between two beam lines is another unique feature of the PSI high intensity proton accelerator facility.

A crucial issue related to a MW-class accelerator is the machine protection system (MPS). The HIPA-MPS get signal from hundreds of diagnostics devices as well as power supplies and is capable of stopping the beam within 5 ms [3].

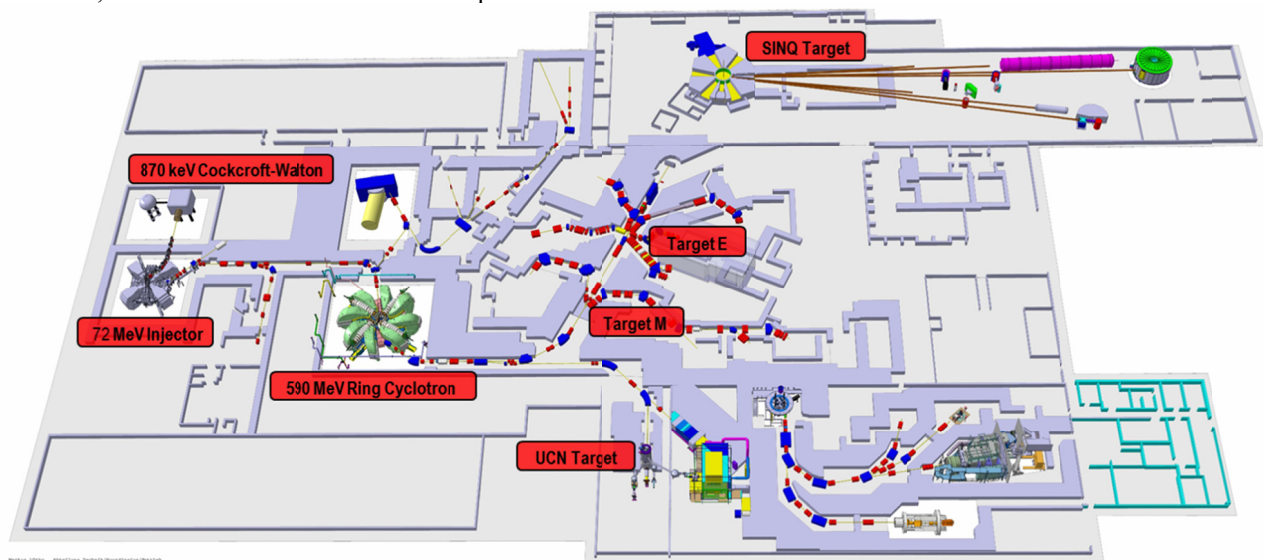


Figure 1: Overview of the PSI high intensity accelerator facility.

<sup>#</sup>davide.reggiani@psi.ch

### EXTRACTION OF A MEGAWATT BEAM

Extraction losses are usually the limiting factor of a high beam power cyclotron. At PSI, at the nominal beam intensity of 2.2 mA, the extraction losses are typically kept below 500 nA, which corresponds to the remarkable efficiency of 99.98%. Extraction losses result from the scattering of halo particles in the electrostatic deflector placed between the orbits of the last two turns. This effect can be minimized by providing a large orbit separation as well as by limiting the size of the beam deflector. Both these methods are followed at the PSI ring cyclotron.

In an isochronous cyclotron the orbit separation is mainly due to two different effects. The most obvious one is the acceleration term that causes a radius increment per turn given by:

$$\frac{dR}{dn_t} = \frac{R}{\gamma(\gamma^2 - 1)} \frac{U_t}{m_0 c^2}$$

where  $U_t$  is the energy gain per turn,  $R$  the orbit radius and  $\gamma$  the relativistic factor. A large turn separation can therefore be obtained by building a large radius machine and by furnishing it with a powerful RF-system. In this way a large  $U_t$  can be achieved or, respectively, a small number of turns  $N_t$ . On the other hand, the relativistic term  $\gamma(\gamma^2 - 1)$  disfavours the radius increment as the energy increases, thus limiting the maximum energy of a cyclotron accelerator to roughly 1 GeV.

The extraction parameters of the PSI ring cyclotron are  $R = 4460$  mm,  $U_t \approx 3$  MeV,  $\gamma = 1.63$ . Plugged into the above equation, these figures give a radius increment between last two turns of about 6 mm. This value can be substantially increased by exploiting the betatron motion of the beam around the ideal orbit. In fact, by choosing carefully the injection parameters, the phase of the horizontal betatron oscillation can be tuned in a way that at the location of the extraction deflector three turns overlap while the very last one gets the maximum radial separation. In this way at the PSI ring cyclotron the gap between the last two turns can be raised from 6 to 18 mm.

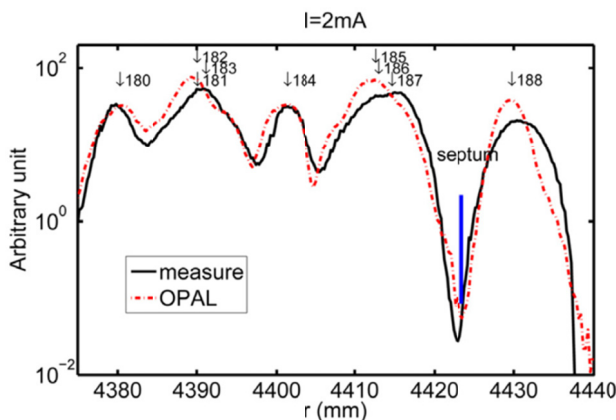


Figure 2: Radial beam profile with turn number at the extraction.

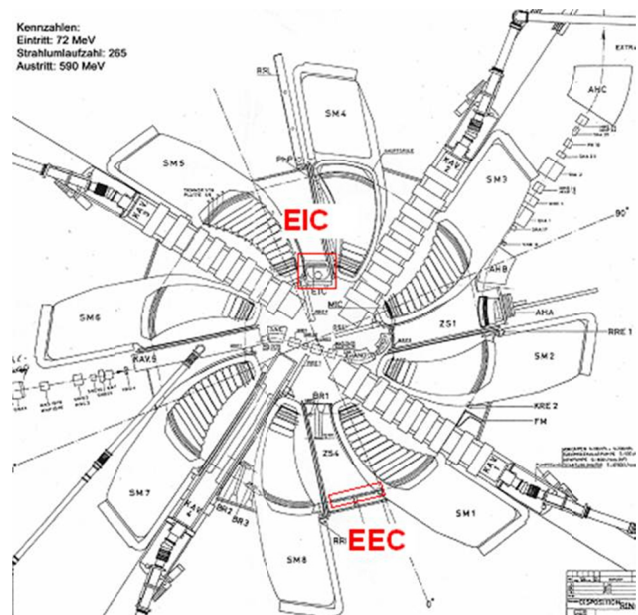


Figure 3: Drawing of the PSI ring cyclotron. The red elements are the electrostatic injection/extraction channels (EIC/EEC).

Figure 2 shows the measured and the simulated radial beam profile of the last orbits at the location of the extraction deflector. The scheme of three overlapping orbits followed by one separated turn can be recognized. The simulation has been carried out by tracking  $\sim 10^8$  macro particle through the accelerator by mean of the OPAL code [4].

A drawing of the ring cyclotron is shown in Fig. 3. The extraction line consists of the electrostatic extraction channel (EEC) followed by the two sector magnets SM1 and SM2 (with the focusing element FM in between) and by the magnetic transport line composed by the magnetic septum AHA and the AHB bend. The electrostatic element EEC is composed of a series of 50  $\mu$ m thick tungsten stripes placed in-between the last two turns of the ring cyclotron and set to ground potential. Thanks to this very thin structure, beam losses due to scattering are minimized. The cathode is located outside the last turn and operates at a potential of -145 kV. The high voltage gap is 16 mm broad while the effective length is 920 mm. The total deflecting angle is  $\theta_{beam} = 8.2$  mrad.

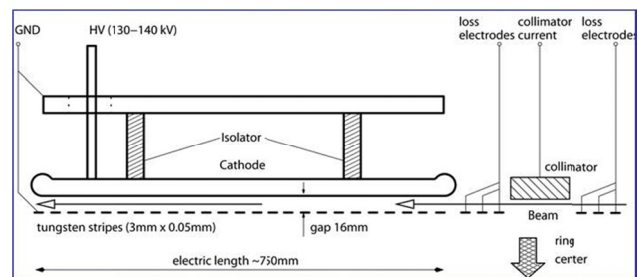


Figure 4: Principle of the electrostatic extraction channel EEC.

## BEAM TRANSPORT FROM THE RING EXTRACTION TO THE SINQ TARGET

After being extracted from the ring cyclotron, the 1.3 MW beam is guided to the meson production targets M and E and eventually to the SINQ spallation source. Figure 5 represents the horizontal ( $x$ ) and vertical ( $y$ ) beam envelopes over the 116 m long transport channel. Light blue elements represent bending magnets while the red ones are quadrupoles. Collimator apertures are depicted by black arrows. Green areas represent the target regions where significant amount of beam is lost. Away from targets, the average loss rate is as low as 1 nA/m (0.6 W/m). This picture was obtained by putting together beam envelope fits of the three beam line sections ring extraction to target M, target M to target E and Target E to SINQ. Such fits are routinely performed at PSI employing the beam profiles measured by over 50 horizontal and vertical beam profile monitors and fitting the  $2\sigma$  beam widths by means of the TRANSPORT computer code [5]. The projected horizontal and vertical beam  $2\sigma$ -emittances, at the extraction in the order of 5 and  $2\pi$  mm·mrad respectively, blow up at target M and E due to multiple Coulomb scattering. At the location of the meson production targets M and E the  $2\sigma$  beam widths are in the order of 1.5 mm and 2.5 mm in  $x$  and  $y$  respectively. Considering a Gaussian beam distribution, this translates to a peak beam power density of almost 200 kW over  $1\text{ mm}^2$ . Target M absorbs 1.6% of beam, without a significant change of the beam energy. The target is composed of a 5 mm thick graphite wheel rotating at a frequency of 1 Hz and shielded against beam misalignment by a Densimet® collimator (Fig. 6).

The beam transport between target M and target E takes place through a dispersion free beam line section

composed of two quadrupole triplets. Two copper collimators are installed respectively 1 m and 2 m downstream of target M in order to shield the beam line components from large angle scattered protons. Between the two triplets and inside the last quadrupole, the vacuum pipe is furnished with four built-in 316L-steel collimators, each of them protecting a beam profile monitor from uncontrolled beam loss. Up to target E, the proton beam transport line is provided with over 30 beam position monitors (BPM). These diagnostics devices are integrated inside an automatic beam position control system which makes use of the BPM signals in order to control a similar number of steering magnets. Furthermore, the beam position and tilt in front of target E can be adjusted by means of a bump formed by three bending magnets.

The design of the meson production target E is similar to the one of target M, but the thickness of the rotating wheel is 8 times larger. This causes beam energy degradation from 590 to 575 MeV. Beam adsorption and losses are also significant. Almost 12% of beam is absorbed by the target material, while about 17% is cut away by a group of four OFHC copper collimators (Fig. 7). This collimation system, installed between target E and the first magnetic element, can be subdivided into two separate subsystems: the first two collimators (KHE0/1) shield the beam line from large angle scattered beam particles, while the second pair (KHE2/3) reshape the proton beam leaving target E in order to match the geometric acceptance of the SINQ beam line. KHE2/3 present an elliptical cross section and a segmented structure made of teeth whose thickness increases along the beam direction. One pair of vertical and horizontal movable slits located respectively 5 and 7 m downstream of KHE3 capture halo particles originating from scattering in KHE2/3.

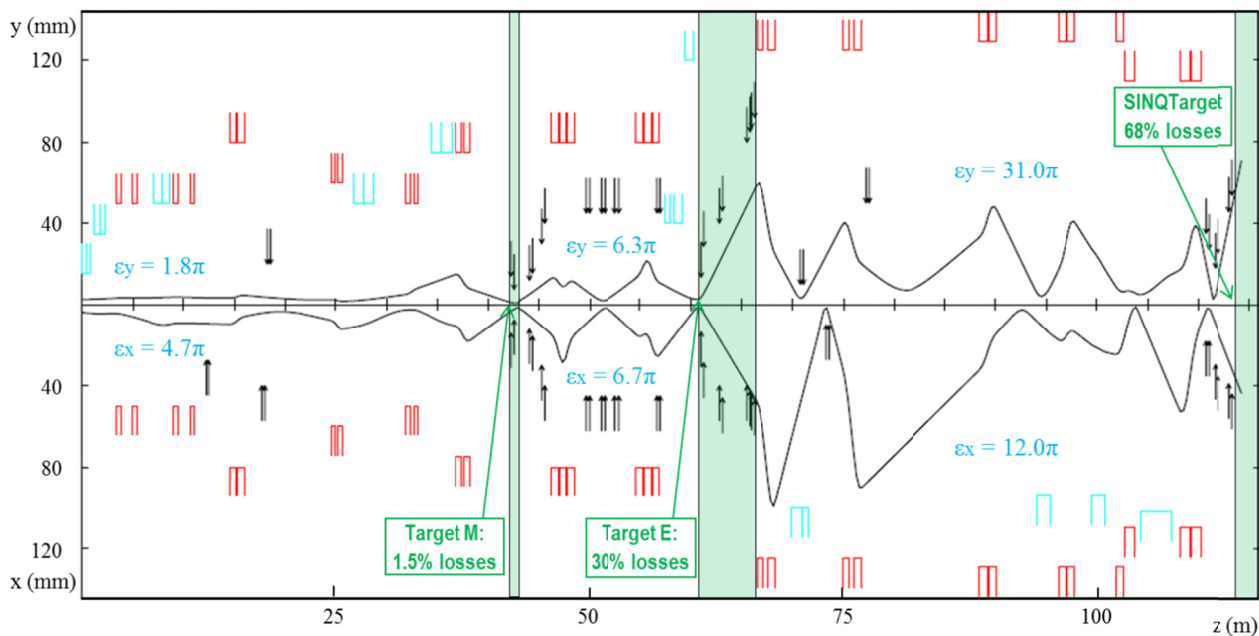


Figure 5: Horizontal and vertical beam envelopes along the PSI high intensity transport line from the ring extraction. Beam emittances ( $2\sigma$ ) are expressed in unit of mm·mrad and refer to the non-dispersive component.

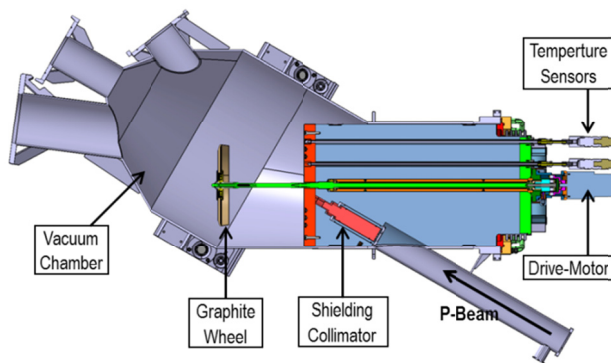


Figure 6: Drawing of the new target M insertion.

Since KHE2 absorbs some 150 kW of beam power, this collimator represents one of the most critical elements of the whole accelerator complex in terms of thermal and mechanical stress as well as activation. In order to better understand the operating limit of KHE2, beam loss and temperature distribution simulations have been recently performed [6]. Moreover, a visual inspection of the collimator was carried out in March 2010 [7].

Up to target M the bending plane is horizontal. On the contrary, SINQ has a vertical bending plane. After leaving the target E region, the beam reaches the dipole magnet AHL that guides the protons downwards, 11 m below the level of target E. Three other bends then turn the beam upwards in the vertical direction in order to reach the SINQ target from the bottom (Fig. 8). The last quadrupole doublet defocuses the beam so that, at the target entrance the beam footprint presents an elliptical cross section with  $2\sigma_x = 44$  mm and  $2\sigma_y = 58$  mm. Three copper collimators installed immediately before the end of the beam line shield the rim of the target entrance window and, at the same time, prevent activation of the beam line component from back scattered neutrons. A review of the SINQ target can be found in [8].

The  $x$  and  $y$  beam distributions at the SINQ target entrance can be described by roughly Gaussian functions with tails cut short by the KHE2/3 collimators (Fig. 9, top). Heat load and mechanical stress generated on the target by such an uneven current distribution are of course very far from the ideal conditions provided by a uniform beam. Since a 1.8 MW upgrade campaign has been launched at PSI-HIPA [9], simulations are being carried out aiming to achieve a more homogeneously distributed

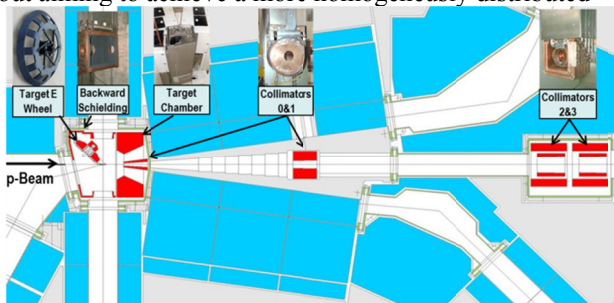


Figure 7: The target E region.

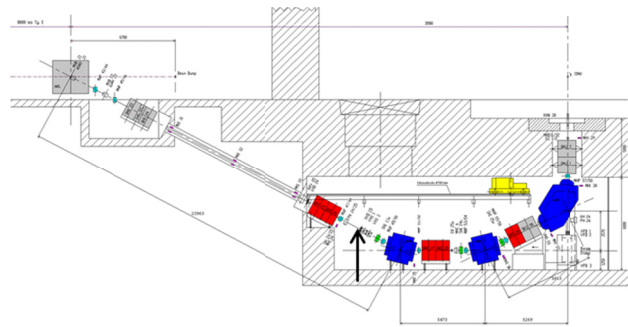


Figure 8: SINQ beam line section from the bending magnet AHL to the SINQ target. The black arrow (upstream of the blue AHM bend) indicates a possible location of a beam rotation system.

beam, in a way which is compatible with the present installation. The common solution of using non linear magnetic elements like octupoles and dodecapoles does not seem to be suitable, as the beam footprint would be distorted. An alternative idea is to wobble the beam on the SINQ target by means of a fast beam rotation, at a frequency of around 100 Hz. Since the last half of the beam line is already completely filled with elements, a possible location for the beam rotation system could be some 24 m away from the SINQ target just upstream of the short horizontal beam line section (Fig. 8). The distribution obtainable by means of the beam rotation was simulated using the ray tracing code TURTLE [10]. The whole beam line from target E to SINQ was included in the simulation. The beam rotation magnets, located 2.5 m upstream of the AHM bend, kick the beam radially by 4.5 mrad. The amplitude of the kick was chosen so that the beam losses on the SINQ collimators are not significantly larger than in the standard case.

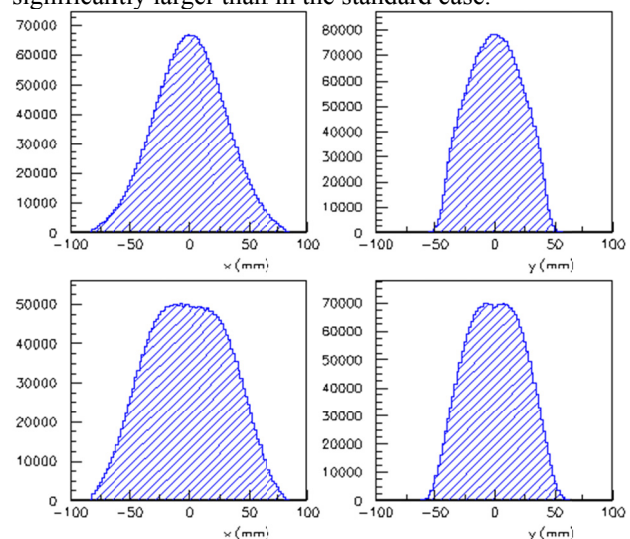


Figure 9: TURTLE Simulation of the proton beam transverse distribution at the SINQ target entrance in normal running conditions (top) and applying a beam rotation system  $\sim 24$  m upstream of the SINQ target (bottom).  $x$  and  $y$  coordinates follow the TURTLE convention ( $x$  is the bending plane) and are therefore reversed.

This procedure was repeated 36 times with an azimuthal step of  $10^\circ$  in order to cover the whole circumference. Results are shown in the two plots in the bottom part of Fig. 9 while the two upper plots represent the beam distribution during standard running conditions. The initial number of particles is the same in both cases (3.6 millions). This simulation shows that by means of the beam rotation technique, the current density in the central  $\text{cm}^2$  of beam at the SINQ target entrance would be reduced by 50%.

## THE UCN BEAM LINE

Since August 2011, the UCN spallation source has operated at PSI-HIPA. The concurrent operation of UCN and SINQ is made possible by a pulsing system that switches the entire 1.3 MW beam between SINQ and UCN beam lines with a duty cycle of 1%. Typical pulse length is 6 s, with a maximum allowed length of 8 s. During the UCN pulse, neutrons arising from the target are first thermalized in liquid  $\text{D}_2\text{O}$  and then cooled down to UCN in a deuterium crystal kept at 5 K. The generated ultra-cold neutrons are stored in a tank and eventually guided to the experiments. The heart of the beam switching system is a small, air-cooled, fast kicker magnet installed about 12 m after the ring extraction point. The 6 mrad tilt given by the kicker produces a 40 mm horizontal displacement seven meters downstream, thus allowing the beam to enter a magnetic septum and get diverted into the UCN beam line. During the transition, the beam is absorbed by a tungsten collimator installed on the upstream end on the septum. In order to limit activation, the switchover time has to be kept as short as possible. For this reason, the timing of the kicker power supply has been tuned so that the first 85% of the beam angular deflection is reached within 1 ms. Under these conditions, considering a UCN operation of one pulse every 200 s without interruptions over one year, calculations have shown that, after 15 days decay time, the collimator dose rate should not exceed 65 mS/h at a distance of 3 cm from its surface. Since nevertheless instantaneous losses on the collimator are too large for the machine protection system, in order to prevent beam trips interlock thresholds of the several beam loss monitors have to be substantially raised for 3 ms starting from the beginning of each kick.

The actual UCN transport line begins at the location of the septum and guides the beam over 46 m towards the UCN source. Ten meters upstream of the target, the beam is blown up by a quadrupole magnet and then collimated so that at the target entrance it gets a circular footprint with a  $4\sigma$  diameter of 160 mm.

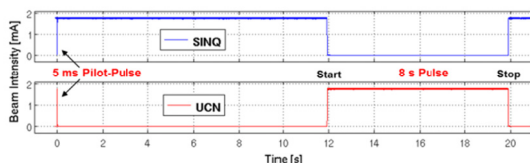


Figure 10: The first 8 s long megawatt UCN beam pulse.

The kicking scheme includes at least one 7 ms short pilot pulse before each long UCN production pulse. This procedure was implemented in order to check that the proton beam is well centred already at the start of production pulse. During the pilot pulse, the beam position is measured by 14 BPMs and 4 harp monitors. If the beam displacement exceeds the tolerance level, a centring step is performed and a new pilot pulse is carried out.

The commissioning of the UCN started in 2008 and lasted three years. Since during this time the UCN source was not yet ready, the beam line was developed and tested by employing a small beam dump installed for this purpose downstream of the last bending magnet. In December 2010, the first 8 s long megawatt beam pulse was shot to the UCN target (Fig. 10).

## CONCLUSION

Extraction and transport of the 1.3 MW proton beam are very well established operations at the PSI HIPA complex. In view of the future 1.8 MW upgrade, particular attention has to be paid to crucial aspects like extraction losses, beam collimation after target E and beam distribution on the SINQ target.

## REFERENCES

- [1] M. Seidel et al., "Production of a 1.3 MW proton beam at PSI", IPAC 2010, Kyoto, Japan, May 23-28, 2010.
- [2] D. Reggiani et al., "A macro-pulsed 1.2 MW beam for the PSI ultra-cold neutron source", PAC09, Vancouver, Canada, May, 4-9, 2009.
- [3] A. Mezger and M. Seidel, "Control and protection aspects of the megawatt proton accelerator at PSI", HB2010, Morschach, Switzerland, September 27 - October 1, 2010.
- [4] Y.J. Bi et al., "Challenges in simulating MW beams in cyclotrons", HB2010, Morschach, Switzerland, September 27 - October 1, 2010.
- [5] U. Rohrer, Graphic Transport Framework, [http://aea.web.psi.ch/Urs\\_Rohrer/MyWeb/trans.htm](http://aea.web.psi.ch/Urs_Rohrer/MyWeb/trans.htm)
- [6] Y. Lee et al, "Simulation based optimization of a collimator system at the PSI proton accelerator", IPAC 2010, Kyoto, Japan, May 23-28, 2010.
- [7] Y. Lee et al, "Visual inspection of a copper collimator irradiated by 590 MeV protons at PSI", HB2010, Morschach, Switzerland, September 27 - October 1, 2010.
- [8] W. Wagner, "PSI's experience with high-power target design and operation", 3rd High-Power Targetry Workshop, Bad Zurzach, Switzerland (2007)
- [9] M. Seidel et al., "Towards the 2 MW cyclotron and latest development at PSI", CYCLOTRONS2010, Lanzhou, China, September 6-10, 2010.
- [10] U. Rohrer, Graphic Turtle Framework, [http://aea.web.psi.ch/Urs\\_Rohrer/MyWeb/turtle.htm](http://aea.web.psi.ch/Urs_Rohrer/MyWeb/turtle.htm)